SCIENTIFIC REPORTS

OPEN

SUBJECT AREAS:
HEART FAILURE
AGEING

Received
28 August 2014

Accepted
19 November 2014

Published
11 December 2014

Correspondence and requests for materials should be addressed to S.-Q.W. (wsq@pku.edu.cn) or G.J. (gj28@ibp.ac.cn)

* These authors contributed equally to this work.

Functional Role of Calstabin2 in Age-related Cardiac Alterations

Qi Yuan[1,3]*, Zheng Chen[2]*, Gaetano Santulli[3]*, Lei Gu[1], Zhi-Guang Yang[1], Zeng-Qiang Yuan[1], Yan-Ting Zhao[4], Hong-Bo Xin[5], Ke-Yu Deng[5], Shi-Qiang Wang[4] & Guangju Ji[1]

[1]National Laboratory of Biomacromolecules, Institute of Biophysics, Chinese Academy of Sciences, Beijing, China, [2]School of Life Sciences, Northeast Normal University, Changchun 130024, PR China, [3]Department of Physiology and Cellular Biophysics, Wu Center for Molecular Cardiology, Columbia University Medical Center, College of Physicians & Surgeons, New York, NY (USA), [4]State Key Laboratory of Biomembrane and Membrane Biotechnology, College of Life Sciences, Peking University, Beijing, China, [5]Institute of Translational Medicine, Nanchang University, Honggu District, Nanchang, China.

Calstabin2 is a component of the cardiac ryanodine receptor (RyR2) macromolecular complex, which modulates Ca^{2+} release from the sarcoplasmic reticulum in cardiomyocytes. Previous reports implied that genetic deletion of Calstabin2 leads to phenotypes related to cardiac aging. However, the mechanistic role of Calstabin2 in the process of cardiac aging remains unclear. To assess whether Calstabin2 is involved in age-related heart dysfunction, we studied Calstabin2 knockout (KO) and control wild-type (WT) mice. We found a significant association between deletion of Calstabin2 and cardiac aging. Indeed, aged Calstabin2 KO mice exhibited a markedly impaired cardiac function compared with WT littermates. Calstabin2 deletion resulted also in increased levels of cell cycle inhibitors p16 and p19, augmented cardiac fibrosis, cell death, and shorter telomeres. Eventually, we demonstrated that Calstabin2 deletion resulted in AKT phosphorylation, augmented mTOR activity, and impaired autophagy in the heart. Taken together, our results identify Calstabin2 as a key modulator of cardiac aging and indicate that the activation of the AKT/mTOR pathway plays a mechanistic role in such a process.

Aging is a major independent risk factor for cardiovascular-related morbidity and mortality. Cardiovascular disease remains the greatest threat to health worldwide, especially in developed countries, and requires long-term medical attention in the elderly[1].

Growing evidence indicates that tissue prematurely age under certain conditions and that disturbances of Ca^{2+} dynamics due to sarcoplasmic reticulum (SR) leak results in several age-related disorders including heart failure, left ventricular hypertrophy, and muscle weakness[2,3]. Cardiac aging is associated with blunted response to aberrant Ca^{2+} handling[1,4], which is an important contributor to the electrical and contractile dysfunction reported in heart failure[5,6]. However, the specific molecular mechanisms underlying abnormal Ca^{2+} handling in cardiac aging remain poorly understood. Recent studies indicate that alterations in SR Ca^{2+} release units occur in aging ventricular myocytes and raise the possibility that impairment in Ca^{2+} release may reflect age-related alterations[3,7]. Calstabin2, also known as FK506 binding protein 12.6 (FKBP12.6)[8], is a small subunit of the cardiac ryanodine receptor (RyR2) macromolecular complex, a major determinant of intracellular Ca^{2+} release in cardiomyocytes, required for excitation-contraction (E-C) coupling[3]. Calstabin2 selectively binds to RyR2 and stabilizes its closed state preventing a leak through the channel[9]. Removal of Calstabin2 from RyR2 causes an increased Ca^{2+} spark frequency, altered Ca^{2+} spark kinetics[10], and can lead to cardiac hypertrophy, which is a prominent pathological feature of age-related heart dysfunction[9,11]. On the other hand, enhanced Calstabin2 binding to RyR2 has been shown to improve myocardial function and prevent cardiac arrhythmias[8,12]. Furthermore, previous reports indicated that Calstabin1, which shares 85% sequence identity with Calstabin2[13], binds to rapamycin and inhibits the activity of the mammalian target of rapamycin (mTOR), a widely recognized master regulator of aging[14], suggesting that Calstabin2 could play a mechanistic role in the process of cardiac aging, not examined hitherto.

We identified Calstabin2 as a regulator of cardiac aging and pointed out the activation of the mTOR pathway followed by compromised autophagy as essential mechanisms involved in such a process.

Results

Genetic deletion of Calstabin2 causes aging related alteration of hearts. To assess whether Calstabin2 is involved in cardiac aging and age-related heart dysfunction, we performed *in vivo* echocardiographic studies

in mice of different age with genetic deletion of Calstabin2. We observed that young (12-week-old) Calstabin2 KO mice exhibited markedly larger hearts (Fig. 1A–C) than WT littermates, without significant differences in heart rate. The left ventricular mass (LVM) in KO mice was 22% higher than in control WT mice (from 84.15 ± 2.02 mg to 102.85 ± 6.44 mg, n = 6, $p < 0.05$, Fig. 1B), and the left ventricular posterior wall at diastole (LVPWd) was increased from 0.81 ± 0.03 mm to 0.95 ± 0.04 mm ($p < 0.05$, Fig. 1C). We also observed that young Calstabin2 KO mice exhibited markedly larger myocyte cross-sectional area and higher heart weight/tibia length (HW/TL) ratios than WT littermates (Supplementary Fig. 1). Accordingly, we observed a significantly different cardiac function in young mice when detecting left ventricular ejection fraction (EF, WT vs KO: 60.02 ± 1.9% vs 67.08 ± 2.0%; $p < 0.05$, Fig. 1D) and fractional shortening (FS, WT vs KO: 31.44 ± 1.3% vs 36.54 ± 1.4%; $p < 0.05$, Fig. 1E).

In contrast, the hearts of aged Calstabin2 null mice did not exhibit any further increase in LVM (Fig. 1B and C), myocyte cross-sectional area, and HW/TL ratio (Supplementary Fig. 1). Strikingly, the value of EF and FS decreased by 36.0% (WT vs KO: 56.1 ± 1.9% vs 35.9 ± 2.0%; $p < 0.01$, n = 6, Fig. 1D) and 30.0% (WT vs KO: 31.1 ± 1.4% vs 21.8 ± 1.5%; $p < 0.01$, Fig. 1E), respectively, in aged Calstabin2 KO mice, indicating that aged Calstabin2 null mice exhibit an impaired heart function.

Next, we examined the effects of Calstabin2 deletion on myocardial remodeling and we found a normal cardiac structure without clear histological differences between young WT and KO mice (Fig. 2A, upper). In contrast, aged Calstabin2 null mice exhibited

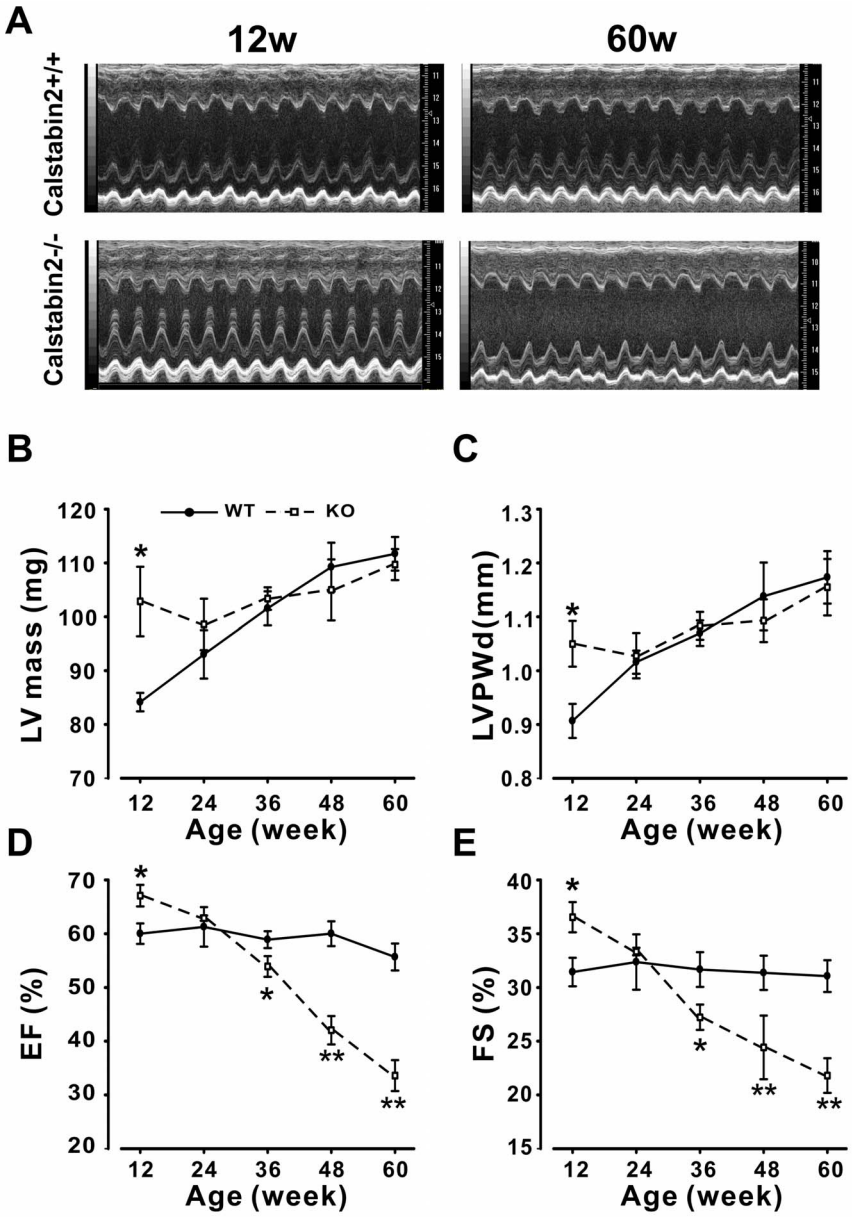

Figure 1 | Calstabin2 KO mice exhibit age-dependent heart dysfunction. (A), Representative echocardiographic (M-mode) photographs from 12- and 60- week-old mice. (B), Echocardiographic measurement of the left ventricle mass (LV mass) at 12, 24, 36, 48 and 60–week-old Calstabin2 KO and WT littermates. LV mass was 22% higher in 12w KO mice than in WT mice, but the aged KO mice displayed similar LV mass, compared to the WT littermates. (C), Ultrasound assessment of left ventricular posterior wall at diastole (LVPWd) in KO and WT mice. (D), Echocardiographic analyses of the ejection fraction (EF). Notably, EF was greatly elevated at the age of 12 weeks, but decreased at 36, 48 and 60 weeks compared to WT littermates. (E), Echocardiographic evaluation of fractional shortening (FS) in 12, 24, 36, 48 and 60–week-old KO and WT littermates. Data are presented as the means ± s.e.m.; n = 6 to 8 per group; *$p < 0.05$, **$p < 0.01$.

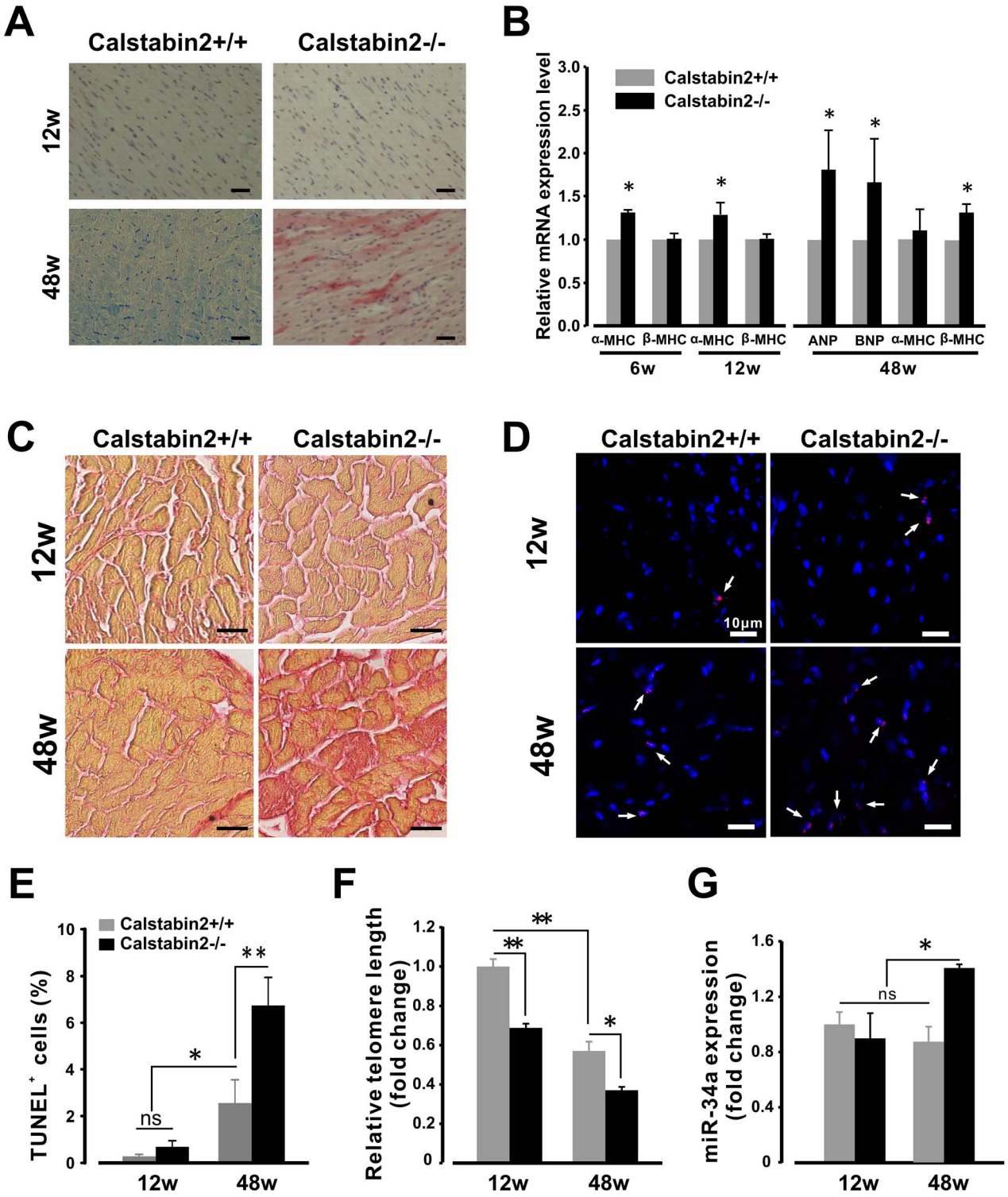

Figure 2 | Aged Calstabin2-null mice display cardiac remodeling. (A), Cardiac sections from young and old WT and KO mice were stained with hematoxylin-eosin. Bar = 100 μm. (B), mRNA levels of α-MHC, β-MHC, ANP, and BNP were determined by real-time RT-qPCR. The expression of α-MHC was remarkably increased in cardiomyocytes from 6 week-and 12-week-old KO mice, respectively; whereas, the expression of ANP, BNP, and β-MHC was significantly increased in 45- to 60-week-old KO mice compared to WT controls. (C), Representative Sirius red staining in transverse heart sections from young and aged Calstabin2 KO mice and WT littermate controls. Hearts from 48-week-old KO mice exhibited increased fibrosis. Bar = 25 μm. (12–15 fields of view were counted per each sample) (D), Representative images of terminal deoxynucleotidyl transferase dUTP nick end labelling (TUNEL) staining of heart sections from 12- and 48-week-old Calstabin2 KO mice and their littermates. As indicated by white arrows, aged Calstabin2 KO hearts exhibited significantly higher numbers of TUNEL-positive cells (arrows); Bar = 10 μm. (E), Quantification of cell death using TUNEL in the hearts of 12- and 48-week-old Calstabin2 KO and WT littermates (12–15 fields of view were counted per each sample) (F), Telomere length measured in young and aged hearts. (G), Quantitative real-time RT-qPCR products for miR-34a in hearts from 12 and 48-week-old Calstabin2 KO and WT littermates. Data are presented as the means ± s.e.m; n = 6 to 8 per group; *p < 0.05, **p < 0.01.

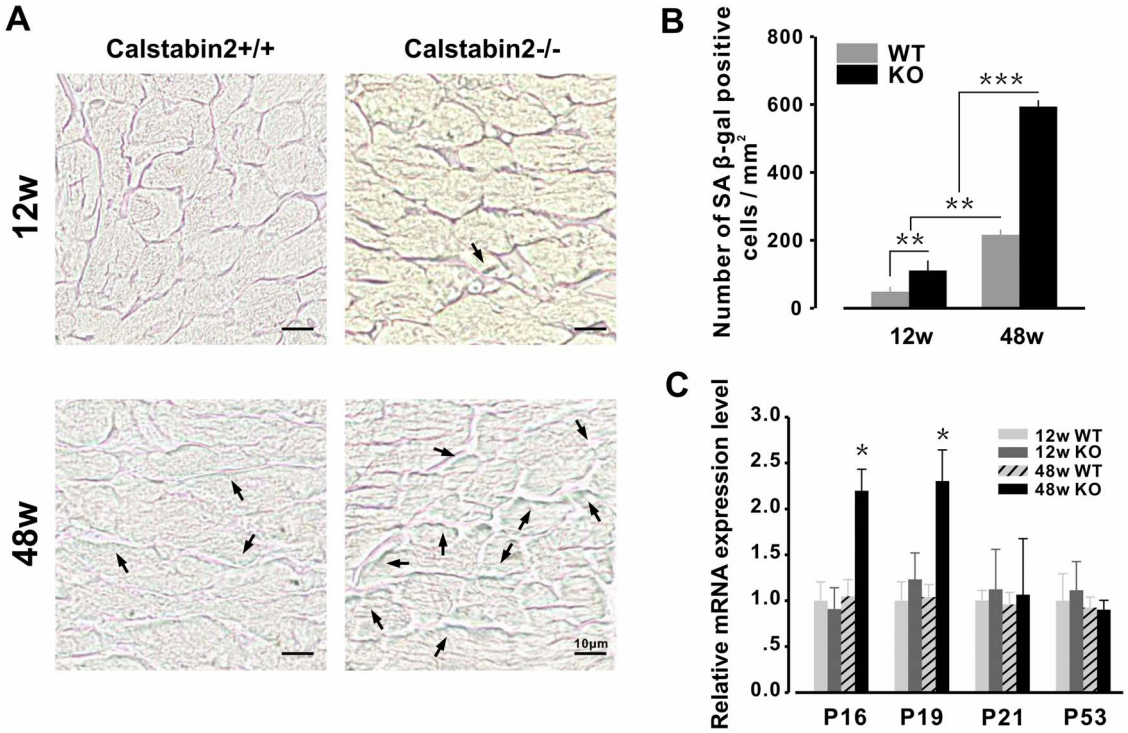

Figure 3 | Calstabin2-null mice exhibit increased cellular senescence. (A), Cardiac sections were analyzed for SA β-gal staining (arrows). The deletion of Calstabin2 leads to significant increase in SA β-gal activity in both young and aged mice. Scale bar = 10 μm. (B), Quantification of SA β-gal positive cells in young and aged mice. (C), mRNA transcript levels of the cell cycle inhibitors p16, p19, p21 and p53, as determined by real-time RT-qPCR. p16 and p19 were significantly increased in aged KO mice. n = at least 5 per group; *$p < 0.05$, **$p < 0.01$ and ***$p < 0.001$.

large areas of cell death (Fig. 2A, lower). Notably, RyR2 distribution was normal in cardiomyocytes from both young and aged KO and WT littermates (Supplementary Fig. 2). RT-qPCR assay revealed that the expression of atrial natriuretic peptide (ANP), brain natriuretic peptide (BNP), and β-myosin heavy chain (MHC) was 82%, 67%, and 32% higher, respectively, in old KO mice compared to age-matched WT littermates (Fig. 2B). Significantly, the mRNA level of α-MHC was increased by 33% and 28% in cardiomyocytes from 6- and 12-week-old KO mice, respectively (Fig. 2B).

Calstabin2 deletion promotes cardiac aging in mice. The above results suggest that deletion of Calstabin2 leads to age-related alteration of cardiomyocytes. To further examine this particular aspect we conducted a series of experiments related to cardiac aging. As depicted in Fig. 2C, in young animals there was no significant difference between WT and KO (3.25 ± 0.18 vs 3.28 ± 0.24%), whereas aged Calstabin2 null mice exhibited a markedly increased fibrosis (17.62 ± 0.33%) compared to age-matched WT animals (9.29 ± 0.30%, $p<0.05$). Since apoptosis is a fundamental feature of aging hearts[15], we performed a TUNEL assay on heart sections, and we found that aged KO hearts exhibited significantly higher rates of cell death compared to WT littermates (6.7 ± 1.2% vs 2.3 ± 0.9%, $p<0.01$) whereas young KO and WT hearts exhibited comparable low rates of cell death (0.7 ± 0.2% vs. 0.3 ± 0.1%, $p>0.05$, Fig. 2D and E).

Telomere length is a marker of aging, and short telomeres are associated with age-related dysfunction, decreased lifespan, and increased mortality[16–18]. As shown in Fig. 2F, the telomeres of the hearts from young KO mice were 31% shorter compared to WT littermates; the telomere length in the hearts of aged WT mice was 43% shorter than that of young WT mice. Furthermore, the telomere length of aged Calstabin2 null mice was significantly reduced compared to WT controls. Recently, microRNA (miR)-34a has been demonstrated to be important in the cardiac aging process[19], playing a critical role in senescence and apoptosis. In our murine model we found that miR-34a levels were not altered in the hearts of young WT or KO mice (Fig. 2G). However, miR-34a expression was significantly up-regulated in the hearts of aged KO mice (Fig. 2G).

To assess cellular senescence, we evaluated the β-galactosidase (SA β-gal) activity and the expression of cell-cycle inhibitors. The results indicate that the number of SA β-gal-positive cells increased with aging (Fig. 3A and B). However, such increase was significantly much higher in 45- to 60-week-old KO compared to WT hearts. Moreover, consistent with previous findings[20], mRNA levels of the cell-cycle inhibitors p16 and p19 but not p21 or p53 were significantly increased in aged KO mice (Fig. 3C). Thus, these data confirm that the deletion of Calstabin2 accelerates cardiac aging.

Calstabin2 deletion causes age-dependent RyR2 channel leak and activation of AKT-mTOR signaling pathway in cardiomyocytes. Previous studies indicated that intracellular Ca^{2+} leak via RyR2 channel results in several age-related disorders[21–23] and the mTOR signaling pathway has been considered among the main drivers for aging[14]. Therefore, we sought to examine such a pathway in our animal models.

Young KO ventricular myocytes exhibited SR Ca^{2+} loads similar to those observed in WT cardiomyocytes (Supplementary Fig. S3). Resting $[Ca^{2+}]_i$ and calcineurin activity did not significantly differ between cardiomyocytes from young WT and KO mice (Fig. 4A and B). However, in aged KO mice, ventricular myocytes exhibited increased Ca^{2+} spark frequency and decreased SR Ca^{2+} loads (Supplementary Fig. S3). The resting $[Ca^{2+}]_i$ of aged KO myocytes increased by 20% [from 0.992 ± 0.013 (n = 87 from at least 4 mice) to 1.217 ± 0.036 (n = 45 from at least 4 mice), $p < 0.001$], indicating that RyR2 channel leak occurs in the aged cardiomyocytes due to Calstabin2 deletion. Concomitantly, calcineurin activity in aged Calstabin2 null mice was increased by 48% (Fig. 4B) compared with WT controls.

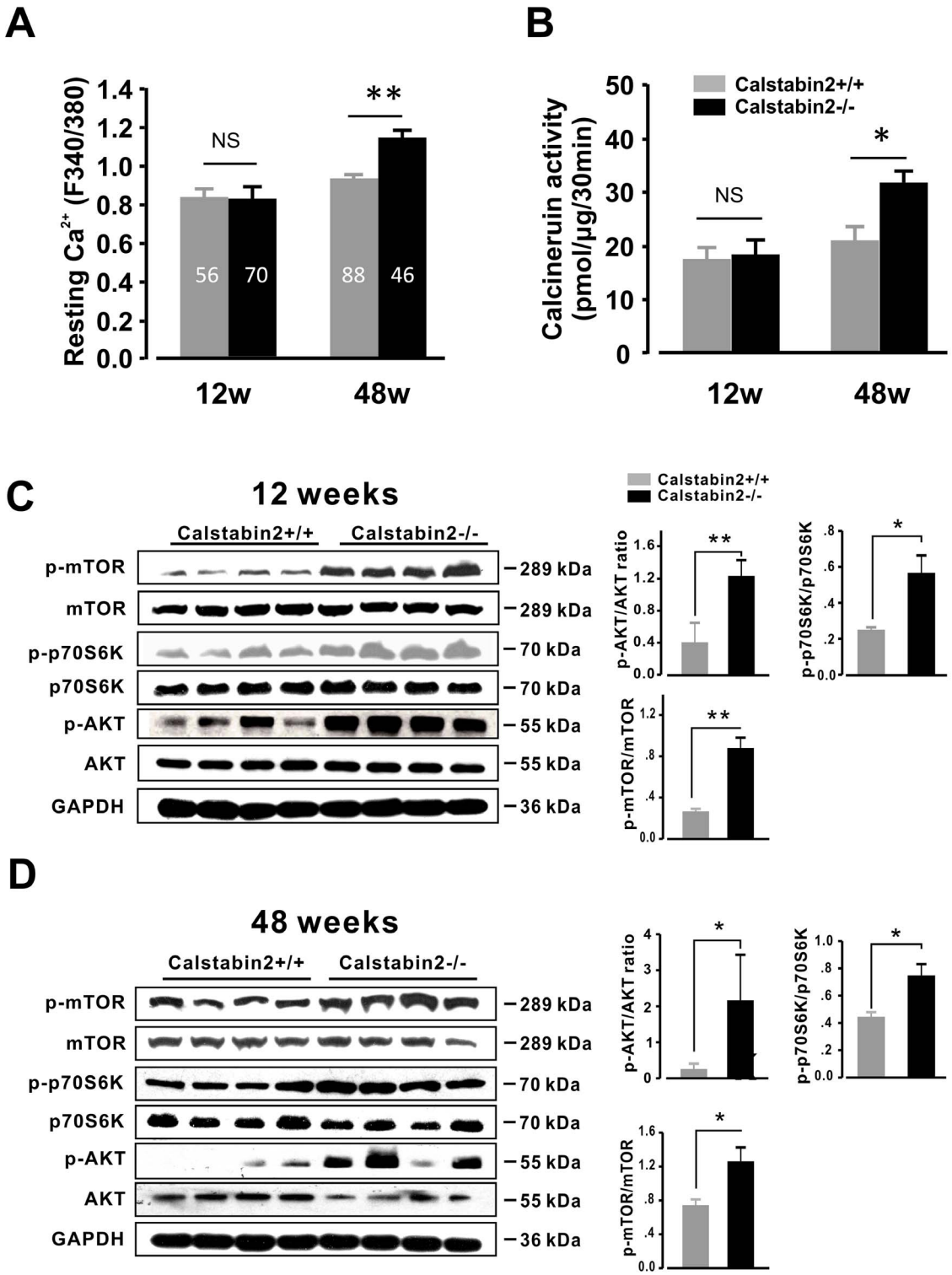

Figure 4 | Depletion of Calstabin2 causes intracellular Ca^{2+} leakage, activation of calcineurin and AKT-mTOR pathway. (A), Resting Ca^{2+} determined by the ratio of F340/F380 fluorescence in WT and KO mice at different ages. At 48 weeks, resting $[Ca^{2+}]_i$ was 20% higher in KO cells than in WT controls. Numbers in the bars indicate the number of the analyzed cells isolated from five to six mice. (B), Calcineurin activity was 48% higher in aged KO mice than in the age-matched WT mice and 1.8-fold higher than in young KO mice. Immunoblots for proteins involved in AKT-mTOR signaling pathway in hearts from 12-week-old (C) and 48-week-old (D) mice. The graphs indicate the relative expression levels of p-AKT, p-p70S6K and p-mTOR. n = 5 per group. Quantitative data are shown as means ± SEM. *P<0.05, **P<0.01 vs WT.

Next, we examined in our model an established key modulator of aging and lifespan: the AKT/mTOR pathway[20,24,25]. We found a three-fold increase in p-AKT levels in young KO hearts (Fig. 4C) indicating that the AKT pathway contributes, at least in part, to cardiac hypertrophy in young Calstabin2 null mice. In aged mice, the level of phosphorylated AKT increased approximately 8.5-fold (Fig. 4D) in the hearts of Calstabin2 null mice. Equally important, mTOR, an important downstream effector of AKT signaling[14], was

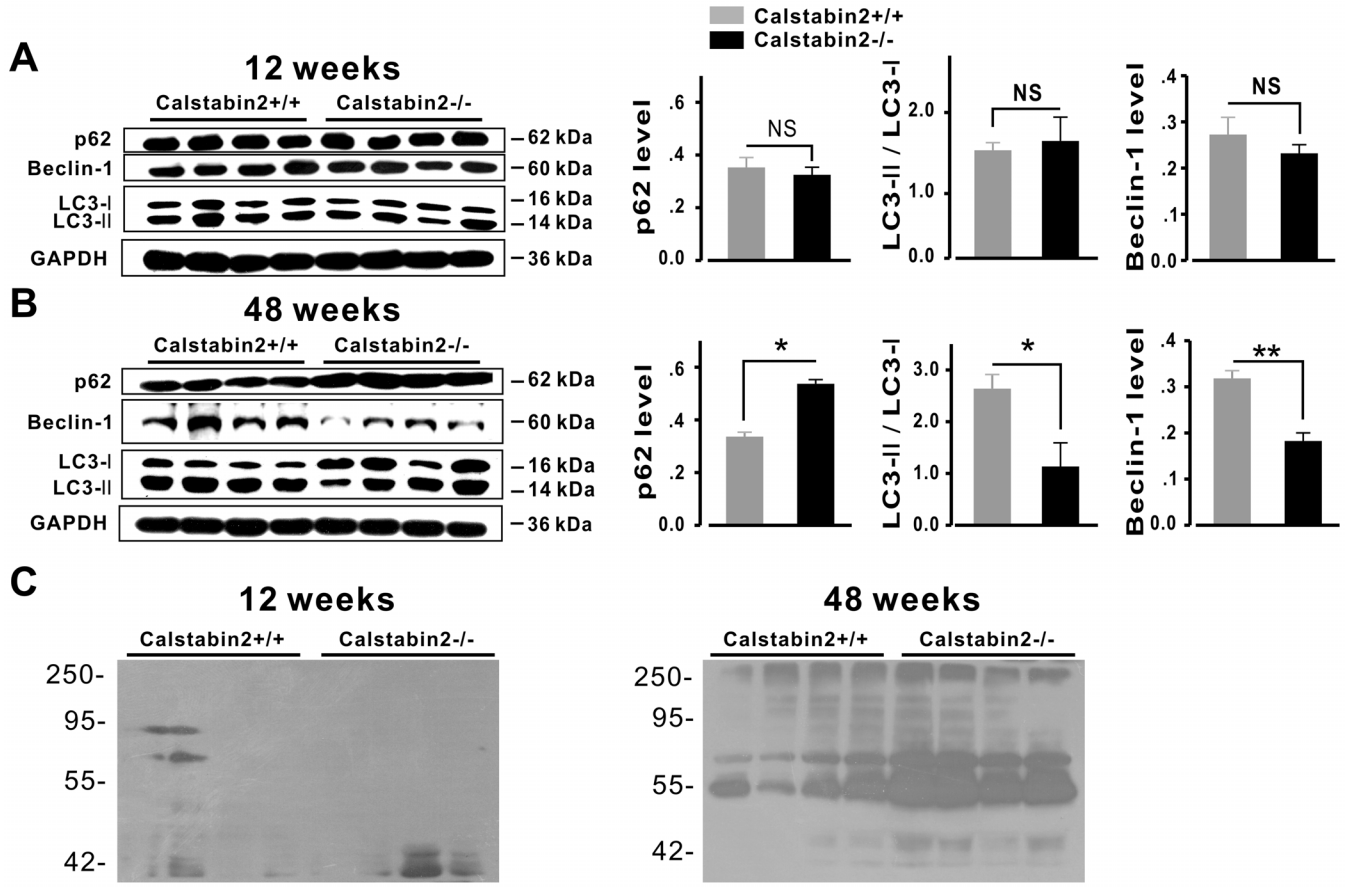

Figure 5 | Deletion of Calstabin2 impairs autophagy in cardiomyocytes of mice. Immunoblots for proteins related to autophagy in hearts from 12-week-old (A) and 48-week-old (B) mice. The graphs indicate the relative levels of p62, LC3-II/LC3-I and Beclin-1. Note that p62 level was increased by 1.7-fold whereas the ratio of LC3-II/LC3-I and the level of Beclin-1 were remarkably decreased in 48-week-old KO mice compared to WT controls. (C), Immunoblots showing poly-ubiquitined proteins in hearts. Note that deletion of Calstabin2 causes a marked accumulation of poly-ubiquitined proteins in 48-week-old KO cardiomyocytes compared with 12-week-old WT hearts. n = 4 per group. Data are shown as the means ± s.e.m. *$p < 0.05$ and **$p < 0.01$.

activated (Fig. 4C and D). The mTORC1 signaling activity and one of its target proteins, p70S6K, were markedly increased in both young and aged KO mice (Fig. 4C and D).

Calstabin2 deletion impairs autophagy system followed by cardiac aging. Given the crucial role of mTOR in regulating autophagy and the essential role of autophagy in aging[26], in the next experiments we assessed the expression of common markers of autophagy p62, LC3-I/II and Beclin-1 in Calstabin2-/- and WT hearts (Fig. 5A and B). Young KO hearts exhibited a similar expression level of p62 and Beclin-1, and the LC3-II-to-LC3-I ratio was not altered when compared to age-matched WT (Fig. 5A). In contrast, aged KO mice displayed increased p62 level, significantly lowered LC3-II to LC3-I ratio, and decreased Beclin-1 level (Fig. 5B). Additionally, we observed the accumulation of poly-ubiquitined proteins in aged KO hearts whereas no significant difference was detectable when comparing samples from young mice (Fig. 5C). Taken together, these findings indicate that a reduced or impaired autophagy occur in aged KO cardiomyocytes.

Discussion

Herein, we determined Calstabin2 as a regulator of cardiac aging and identified the activation of the AKT/mTOR pathway followed by compromised autophagy as essential mechanisms involved in such a process. Previous studies indicated that disturbances of $[Ca^{2+}]_i$ due to RyR2 channel leakage result in several age-related disorders[21,27]. We found that genetic deletion of Calstabin2 accelerated cardiac aging, leading to age-related cardiac dysfunction.

Cardiac muscle expresses two distinct myosin heavy chain (MHC) isoforms designated as α and β. The pattern of cardiac MHC isoform expression is extremely dynamic; namely, α-MHC is normally highly expressed in the adult rodent, while β-MHC predominates in early cardiac developmental stage[28]. Here we found that α-MHC gene was up-regulated in young Calstabin2 KO mice and, unexpectedly, the β-MHC gene was significantly increased in aged Calstabin2 KO cardiomyocytes compared with the WT controls suggesting that Calstabin2 is involved in the regulation of the maturation process of the heart.

Cardiac aging includes well-acknowledged features, including impairment of myocardial function, remodeling of cardiomyocyte structure, and increased cardiac fibrosis[11,29]. In the present study, the cardiac function was declined in aged Calstabin2 KO mice compared with age-matched WT littermates, as revealed by ultrasound analysis. This aspect was further confirmed by the increased levels of ANP and BNP, which have been identified as markers of age-related heart dysfunction[1], in aged Calstabin2 KO mice. Our histological studies of the heart indicated that aged Calstabin2 null mice exhibited large areas of cell death and greatly increased myocardial fibrosis, both considered biomarkers of cardiac aging[1], respect to age-matched WT, indicating a strong myocardial remodeling in Calstabin2 null mice.

Mounting evidence indicates that DNA damage and telomeres attrition play important roles in cardiac aging and disease[18,30].

Indeed, fifth-generation telomerase KO mice display severely reduced telomere length and suffer from severe left ventricular failure[30]. Conversely, stabilizing telomeres prevents doxorubicin-induced cardiac apoptosis in WT mice but not in telomerase-deficient mice[31]. Here we demonstrate that genetic deletion of Calstabin2 caused the length of telomeres to be significantly shortened even in young KO mice compared to WT littermates; the telomere length in the hearts of aged KO mice were further reduced compared to WT controls and the young KO mice. Cellular senescence is a well-characterized model of aging[32]. Previous studies clearly demonstrated that cell cycle inhibitors and β-galactosidase (SA β-gal) are senescence-associated biomarkers[20]. Here we found that the relative mRNA expression level of P16 and P19, but not P21 and P53, was significantly up-regulated in aged Calstabin2 KO cardiomyocytes. Our evaluation study on the SA β-gal activity also indicates that the number of SA β-gal-positive cells remarkably increases with aging, and such an increase is significantly much higher in 45- to 60-week-old KO compared to WT hearts. Recent studies have identified the miR-34 family (comprising miR-34a, b, and c) as a critical player in senescence. In particular, miR-34a has been shown to be critical in the cardiac aging process[19]. In the present study we demonstrate that miR-34a expression was significantly up-regulated in the hearts of aged KO mice, further indicating that deletion of Calstabin2 accelerates cardiac aging process. Further investigations are warranted to identify the molecular mechanism linking Calstabin2 and the expression of miR-34a.

The fact that Calstabin2 stabilizes RyR2 Ca^{2+} release channels and inhibits calcineurin activity[33] suggests that cardiac dysfunction might be, at least in part, caused by increased Ca^{2}-dependent calcineurin activity resulting from loss of Calstabin2. This notion is entirely supported by our present findings showing that both resting Ca^{2+} concentration and calcineurin activity were significantly elevated in 45-60 week-old mice. To explain this phenomenon, one important factor should be noted. As Calstabin2 can also bind to and inhibit calcineurin[34], the effect of Calstabin2 deletion on the activity of calcineurin may be masked by the presence of abundant Calstabin1 in young mice. Of course other mechanisms are involved and further investigations are warranted to explore in detail the regulation of Ca^{2+} handling by Calstabin2.

AKT/mTOR signaling has been demonstrated to be crucial in regulating heart growth and hypertrophy, and more in general, aging and lifespan[14,35–37]. Consistent with this view, we found that the hearts of Calstabin2-null mice exhibited increased p-AKT level, suggesting that AKT signaling could be involved in the 'pre-maturity' of the heart in young KO mice. The sustained activation of AKT in aged KO mice resulted in cardiac aging and age-associated impaired cardiac function by the activation of mTOR signaling pathway. Specifically, in our model mTOR was activated in both young and aged Calstabin2 KO cardiomyocytes, implying that the sustained activation of mTOR might result in cardiac aging. These findings are in agreement with the previous demonstration that mTOR inhibition can actually extend lifespan[38]. The same mTOR is also involved in the regulation of autophagy, a conserved cellular process for bulk degradation and recycling of long-lived proteins and damaged organelles to maintain energy homeostasis. In the heart, autophagy is increased in heart failure and in response to stress conditions, including ischemia/reperfusion and pressure-overload[26]. However, whether up-regulation of autophagy under cardiac stress condition is protective or maladaptive is still controversial. Undeniably, under basal condition, constitutive cardiomyocyte autophagy is required for protein quality control and normal cellular structure and function. Reduction of autophagy in the heart has been reported to lead to ventricular dilatation and contractile dysfunction[39], whereas enhancement of autophagy has been shown to prevent cardiac aging in mice[20]. In aged Calstabin2 KO mice the sustained activation of mTOR signaling resulted in marked inhibition of autophagy, as revealed by the dramatic dysregulation of p62, Beclin-1, and LC3-II/LC3-I. The accumulation of poly-ubiquitined proteins in aged KO hearts further corroborates our model of impaired autophagy. Indeed, the accumulation of abnormal proteins and organelles induced by impaired autophagy in aged hearts has been demonstrated recently[40]. Ergo, impaired autophagy is among the mechanisms hastening cardiac aging following the deletion of Calstabin2.

Overall, our data demonstrate the acceleration of the cardiac aging process in Calstabin2-/- mice. Deletion of Calstabin2 leads to cardiac dysfunction and myocardial remodeling in aged mice, and promotes the aging process of the heart, as demonstrated by increased fibrosis, cardiomyocyte apoptosis, shortening of telomere length and augmented cellular senescence. Mechanistically, the absence of Calstabin2 in aged animals is associated with increased calcineurin activity induced by higher intracellular resting Ca^{2+}, hyperactivation of the AKT-mTOR signaling pathway and impaired autophagy.

Methods

Detailed Methods are available in the Supplementary material.

Animal studies. All experiments were performed in accordance with the relevant guidelines and regulation that were approved by the Committee on Animal Care of Institute of Biophysics, Chinese Academy of Sciences, China. Calstabin2 KO (-/-) mice were generated using homologous recombination to disrupt exon 3 of the calstabin2 gene, as previously described[9]. We used Calstabin2-/- male mice backcrossed for at least 12 generations with a 129/Sv/Ev genetic background; age-matched male wild-type (WT) littermates were used as control. The investigators were blinded to the genotype, age and treatment of the groups.

Ultrasound analysis of cardiac function. Mice were anesthetized with 2% inhaled isoflurane. Echocardiography was performed using a VeVo 770 Imaging System (VisualSonics, Toronto, Ontario, Canada) in M-mode with a 12-MHz microprobe as described[41]. Triplicate measurements of cardiac function were obtained from each mouse.

Cardiomyocyte isolation and resting Ca^{2+} measurement. Mice were anesthetized by intraperitoneal injection of pentobarbital sodium (150 mg/kg) and single ventricular cardiomyocytes were enzymatically isolated from adult mice as described previously[42]. Individual cardiomyocytes were incubated with 10 μM Fura-2 AM (Invitrogen) in normal Tyrode solution, containing (in mM): 135 NaCl, 4 KCl, 1.8 $CaCl_2$, 1 $MgCl_2$, 10 HEPES, 1.2 $NaH_2PO_4{\cdot}2H_2O$, 10 glucose, pH 7.36, adjusted with NaOH, for 5 min at 37°C. After loading, the cells were washed several times and transferred to a recording chamber. Photometric measurements were conducted in Tyrode solution using an Olympus cellR system, operated at an emission wavelength of 510 nm, with excitation wavelengths of 340 and 380 nm[2,43]. The relative resting Ca^{2+} level (estimated by a ratio of 340/380 nm) was recorded and data were analyzed using Olympus cellR Software.

Immunoblotting and calcineurin activity. Anesthetized mice were sacrificed immediately and mouse ventricles were harvested and homogenized in RIPA lysis buffer containing a protease inhibitor cocktail (Roche, Basel, Switzerland), proteins were resolved by SDS–PAGE and transferred to PVDF membranes (Millipore, Billerica, MA). See Supplementary material for details. Calcineurin activity was determined as previously described[27].

Immunostaining of RyR2. Isolated mouse cardiomyocytes were initially allowed to attach to 0.5% poly-l-lysine coated coverslips for 1 h and were then fixed in 4% paraformaldehyde for 20 min. Myocytes were washed three times, 5 min per time, in PBS and permeabilized in PBS containing 0.1% Triton-X 100 for 15 min before incubating in blocking buffer (5% BSA in PBS) for 2 h to block non-specific binding of the antibody. Mouse monoclonal anti-RyR antibody (ThermoFisher Scientific) was diluted in blocking buffer (1 : 50) and incubated with ventricular myocytes overnight at 4°C. After washing, secondary antibody (Alexa Fluor 488-conjugated goat anti-mouse IgG, 1 : 1000, Invitrogen) was added to the blocking buffer and incubated with the cells for 1 h, and then washed out. Cells were then mounted on slides and examined using a laser scanning confocal microscope (Leica SP5, 40 × 1.25 NA oil immersion objective). Images were analyzed using FIJI software.

Real-time RT-qPCR. Quantitative real-time RT-qPCR was performed using SYBR® Premix Ex Taq™ II (TaKaRa Bio Inc, Ōtsu, Japan.) in a Corbett 6200 PCR machine (Qiagen, Hilden, Germany) following the manufacturer's instructions. Briefly, total RNA was extracted from frozen tissues using TRIzol reagent (ThermoFisher Scientific). 2 μg of RNA was then reverse transcribed to first-stand cDNA using random primers and M-MLV reverse tanscriptase (Promega, Madison, WI), as described[44]. Primers are reported in Supplementary material.

For the quantification of microRNA-34a, reverse-transcription was performed with the TaqMan® MicroRNA Reverse Transcription Kit using small RNA-specific RT primer. The reactions were incubated at 16°C for 30 min, 42°C for 30 min and

85°C for 5 min, chilled on ice for 5 min, and the cDNA was stored at −20°C. The RT-qPCR was performed with the TaqMan® Small RNA Assay following the manufacturer's instructions as follows: 50°C for 2 minutes, 95°C for 10 minutes, followed by 40 cycles of 95°C for 10 s, 60°C for 60 s. U6 was used as endogenous control to normalize Ct values. microRNA-34a expression was compared by ΔΔCt[44].

Measurement of relative heart telomere length. Genomic DNA was extracted from heart using the DNeasy Blood & Tissue Kit (Qiagen). We assessed the relative heart telomere length using quantitative PCR, by measuring for each sample the relative amount of telomere DNA (t) as compared to the amount of single copy gene (36B4) DNA (s) in the same sample (t/s ratio) (Cawthon, 2002). Real-time RT-qPCR was performed using SYBR® Premix Ex Taq™ II (TaKaRa) in a Corbett 6200 PCR machine (Qiagen). The primers sequences used were as follows:

Telomere:
Forward- GGTTTTTGAGGGTGAGGGTGAGGGTGAGGGTGAGGGT,
Reverse- TCCCGACTATCCCTATCCCTATCCCTATCCCTATCCCTA
36B4:
Forward-CACACTCCATCATCAATGGGTACAA,
Reverse- CAGTAAGTGGGAAGGTGTACTCA

Thermocycling parameters were 95°C for 10 min activation, followed by 40 cycles of 95°C for 15 sec, and 54°C for 60 sec for PCR amplification of telomeric region; 95°C for 10 min activation, followed by 40 cycles of 95°C for 15 sec, and 58°C for 60 sec.

TUNEL analysis. Mice were anesthetized by intraperitoneal injection of pentobarbital sodium (150 mg/kg). Hearts were freshly isolated and quickly cannulated through the aorta and were perfused on a Langendoff apparatus to remove the blood. Hearts were then mounted in a plastic bowl containing OCT (ThermoFisher Scientific), and maintained vertically to ensure the sectioning was performed in a transverse manner. The mounted heart tissues were frozen in isopentane pre-chilled at −159°C for 30 to 40 seconds and stored at −80°C. Transverse sectioning of the muscle tissues was performed using a Leica CM3050S cryostat (Wetzlar, Germany). Heart sections (10 μm) were used to perform the terminal deoxynucleotidyl transferase (TdT)-mediated dUTP nick end-labeling (TUNEL) assay (In-Situ-Cell-Death detection kit, Roche), according to the manufacturer's instructions. The number of TUNEL-positive cells and total cells in heart tissue sections were quantified under the Leica SP5 confocal microscope.

SA β-gal activity. Fresh frozen tissue sections were analyzed for SA β-gal activity according to the manufacturer's protocol (Cell Signaling).

Histology. Hearts were harvested from each group and fixed in 10% phosphate-buffered formaldehyde for 24 hours, dehydrated with ethanol, embedded in paraffin, and sectioned transversely (5 μm), using standard protocols. To measure myocyte cross-sectional area we used Alexa Fluor 488 tagged wheat germ agglutinin staining (Thermo Fisher Scientific, 10.0 μg/mL, with samples incubated in dark for 10 minutes at 37°C)[40,41]. Images were recorded under the Leica SP5 confocal microscope. Sirius red staining was performed as previously described[45] and fibrosis was quantified using FIJI.

Statistical analysis. Statistical analysis was performed using SigmaPlot (Systat Software Inc., San Jose, CA, USA). Values given are means ± s.e.m. Data were tested for significance using the Student's *t* test. Data from three groups were compared by one-way, repeated measures ANOVA and significant differences between groups were determined by the Student–Newman–Keuls test for paired comparisons, unless otherwise indicated. Only results with values of $P < 0.05$ were considered statistically significant.

1. Lakatta, E. G. & Levy, D. Arterial and cardiac aging: major shareholders in cardiovascular disease enterprises: Part II: the aging heart in health: links to heart disease. *Circulation* **107**, 346–354 (2003).
2. Umanskaya, A. *et al.* Genetically enhancing mitochondrial antioxidant activity improves muscle function in aging. *Proc Natl Acad Sci U S A*, doi:10.1073/pnas.1412754111 (2014).
3. Marks, A. R. Calcium cycling proteins and heart failure: mechanisms and therapeutics. *J Clin Invest* **123**, 46–52, doi:10.1172/JCI62834 (2013).
4. Cooper, L. L. *et al.* Redox modification of ryanodine receptors by mitochondria-derived reactive oxygen species contributes to aberrant Ca2+ handling in ageing rabbit hearts. *J Physiol* **591**, 5895–5911, doi:10.1113/jphysiol.2013.260521 (2013).
5. Paavola, J. *et al.* Polycystin-2 mutations lead to impaired calcium cycling in the heart and predispose to dilated cardiomyopathy. *J Mol Cell Cardiol* **58**, 199–208, doi:10.1016/j.yjmcc.2013.01.015 (2013).
6. Eisner, D., Bode, E., Venetucci, L. & Trafford, A. Calcium flux balance in the heart. *J Mol Cell Cardiol* **58**, 110–117, doi:10.1016/j.yjmcc.2012.11.017 (2013).
7. Howlett, S. E., Grandy, S. A. & Ferrier, G. R. Calcium spark properties in ventricular myocytes are altered in aged mice. *Am J Physiol Heart Circ Physiol* **290**, H1566–1574, doi:10.1152/ajpheart.00686.2005 (2006).
8. Huang, F., Shan, J., Reiken, S., Wehrens, X. H. & Marks, A. R. Analysis of calstabin2 (FKBP12.6)-ryanodine receptor interactions: rescue of heart failure by calstabin2 in mice. *Proc Natl Acad Sci U S A* **103**, 3456–3461, doi:10.1073/pnas.0511282103 (2006).
9. Xin, H. B. *et al.* Oestrogen protects FKBP12.6 null mice from cardiac hypertrophy. *Nature* **416**, 334–338, doi:10.1038/416334a (2002).
10. Zhang, X. *et al.* Dissociation of FKBP12.6 from ryanodine receptor type 2 is regulated by cyclic ADP-ribose but not beta-adrenergic stimulation in mouse cardiomyocytes. *Cardiovasc Res* **84**, 253–262, doi:10.1093/cvr/cvp212 (2009).
11. Santulli, G. & Iaccarino, G. Pinpointing beta adrenergic receptor in ageing pathophysiology: victim or executioner? Evidence from crime scenes. *Immun Ageing* **10**, 10, doi:10.1186/1742-4933-10-10 (2013).
12. Gellen, B. *et al.* Conditional FKBP12.6 overexpression in mouse cardiac myocytes prevents triggered ventricular tachycardia through specific alterations in excitation-contraction coupling. *Circulation* **117**, 1778–1786, doi:10.1161/CIRCULATIONAHA.107.731893 (2008).
13. Mustafi, S. M., Chen, H., Li, H., Lemaster, D. M. & Hernandez, G. Analysing the visible conformational substates of the FK506-binding protein FKBP12. *Biochem J* **453**, 371–380, doi:10.1042/BJ20130276 (2013).
14. Santulli, G. & Totary-Jain, H. Tailoring mTOR-based therapy: molecular evidence and clinical challenges. *Pharmacogenomics* **14**, 1517–1526, doi:10.2217/pgs.13.143 (2013).
15. Kashef, F. *et al.* Ankyrin-B protein in heart failure: identification of a new component of metazoan cardioprotection. *J Biol Chem* **287**, 30268–30281, doi:10.1074/jbc.M112.368415 (2012).
16. Missios, P. *et al.* Glucose substitution prolongs maintenance of energy homeostasis and lifespan of telomere dysfunctional mice. *Nat Commun* **5**, 4924, doi:10.1038/ncomms5924 (2014).
17. Armanios, M. Telomeres and age-related disease: how telomere biology informs clinical paradigms. *J Clin Invest* **123**, 996–1002, doi:10.1172/JCI66370 (2013).
18. Terai, M. *et al.* Association of telomere shortening in myocardium with heart weight gain and cause of death. *Sci Rep* **3**, 2401, doi:10.1038/srep02401 (2013).
19. Boon, R. A. *et al.* MicroRNA-34a regulates cardiac ageing and function. *Nature* **495**, 107–110, doi:10.1038/nature11919 (2013).
20. Inuzuka, Y. *et al.* Suppression of phosphoinositide 3-kinase prevents cardiac aging in mice. *Circulation* **120**, 1695–1703, doi:10.1161/CIRCULATIONAHA.109.871137 (2009).
21. Vest, J. A. *et al.* Defective cardiac ryanodine receptor regulation during atrial fibrillation. *Circulation* **111**, 2025–2032, doi:10.1161/01.CIR.0000162461.67140.4C (2005).
22. Gonzalez, D. R., Treuer, A. V., Castellanos, J., Dulce, R. A. & Hare, J. M. Impaired S-nitrosylation of the ryanodine receptor caused by xanthine oxidase activity contributes to calcium leak in heart failure. *J Biol Chem* **285**, 28938–28945, doi:10.1074/jbc.M110.154948 (2010).
23. Alberdi, E. *et al.* Ca(2+) -dependent endoplasmic reticulum stress correlates with astrogliosis in oligomeric amyloid beta-treated astrocytes and in a model of Alzheimer's disease. *Aging Cell* **12**, 292–302, doi:10.1111/acel.12054 (2013).
24. Johnson, S. C., Rabinovitch, P. S. & Kaeberlein, M. mTOR is a key modulator of ageing and age-related disease. *Nature* **493**, 338–345, doi:10.1038/nature11861 (2013).
25. Hua, Y. *et al.* Chronic Akt activation accentuates aging-induced cardiac hypertrophy and myocardial contractile dysfunction: role of autophagy. *Basic Res Cardiol* **106**, 1173–1191, doi:10.1007/s00395-011-0222-8 (2011).
26. Sciarretta, S., Yee, D., Shenoy, V., Nagarajan, N. & Sadoshima, J. The importance of autophagy in cardioprotection. *High Blood Press Cardiovasc Prev* **21**, 21–28, doi:10.1007/s40292-013-0029-9 (2014).
27. Goonasekera, S. A. *et al.* Decreased cardiac L-type Ca(2)(+) channel activity induces hypertrophy and heart failure in mice. *J Clin Invest* **122**, 280–290, doi:10.1172/JCI58227 (2012).
28. Herron, T. J., Korte, F. S. & McDonald, K. S. Loaded shortening and power output in cardiac myocytes are dependent on myosin heavy chain isoform expression. *Am J Physiol Heart Circ Physiol* **281**, H1217–1222 (2001).
29. Sardu, C., Marfella, R. & Santulli, G. Impact of diabetes mellitus on the clinical response to cardiac resynchronization therapy in elderly people. *J Cardiovasc Transl Res* **7**, 362–368, doi:10.1007/s12265-014-9545-9 (2014).
30. Leri, A. *et al.* Ablation of telomerase and telomere loss leads to cardiac dilatation and heart failure associated with p53 upregulation. *EMBO J* **22**, 131–139, doi:10.1093/emboj/cdg013 (2003).
31. Werner, C. *et al.* Effects of physical exercise on myocardial telomere-regulating proteins, survival pathways, and apoptosis. *J Am Coll Cardiol* **52**, 470–482, doi:10.1016/j.jacc.2008.04.034 (2008).
32. Lopez-Otin, C., Blasco, M. A., Partridge, L., Serrano, M. & Kroemer, G. The hallmarks of aging. *Cell* **153**, 1194–1217, doi:10.1016/j.cell.2013.05.039 (2013).
33. Lam, E. *et al.* A novel FK506 binding protein can mediate the immunosuppressive effects of FK506 and is associated with the cardiac ryanodine receptor. *J Biol Chem* **270**, 26511–26522 (1995).
34. Kawamura, A. & Su, M. S. Interaction of FKBP12-FK506 with calcineurin A at the B subunit-binding domain. *J Biol Chem* **270**, 15463–15466 (1995).
35. Lamming, D. W. *et al.* Depletion of Rictor, an essential protein component of mTORC2, decreases male lifespan. *Aging Cell* **13**, 911–917, doi:10.1111/acel.12256 (2014).
36. Wang, X. *et al.* hNAG-1 increases lifespan by regulating energy metabolism and insulin/IGF-1/mTOR signaling. *Aging (Albany NY)* **6**, 690–704 (2014).
37. Santulli, G., Ciccarelli, M., Trimarco, B. & Iaccarino, G. Physical activity ameliorates cardiovascular health in elderly subjects: the functional role of the

beta adrenergic system. *Front Physiol* **4**, 209, doi:10.3389/fphys.2013.00209 (2013).
38. Leontieva, O. V., Paszkiewicz, G. M. & Blagosklonny, M. V. Weekly administration of rapamycin improves survival and biomarkers in obese male mice on high-fat diet. *Aging Cell* **13**, 616–622, doi:10.1111/acel.12211 (2014).
39. Nakai, A. *et al.* The role of autophagy in cardiomyocytes in the basal state and in response to hemodynamic stress. *Nat Med* **13**, 619–624, doi:10.1038/nm1574 (2007).
40. Zhou, J. *et al.* GSK-3alpha is a central regulator of age-related pathologies in mice. *J Clin Invest* **123**, 1821–1832, doi:10.1172/JCI64398 (2013).
41. Santulli, G. *et al.* CaMK4 Gene Deletion Induces Hypertension. *J Am Heart Assoc* **1**, e001081, doi:10.1161/JAHA.112.001081 (2012).
42. Lehnart, S. E., Wehrens, X. H. & Marks, A. R. Defective ryanodine receptor interdomain interactions may contribute to intracellular Ca2+ leak: a novel therapeutic target in heart failure. *Circulation* **111**, 3342–3346, doi:10.1161/CIRCULATIONAHA.105.551861 (2005).
43. Xie, W. *et al.* Imaging atrial arrhythmic intracellular calcium in intact heart. *J Mol Cell Cardiol* **64**, 120–123, doi:10.1016/j.yjmcc.2013.09.003 (2013).
44. Santulli, G. *et al.* A selective microRNA-based strategy inhibits restenosis while preserving endothelial function. *J Clin Invest* **124**, 4102–4114 (2014).
45. Christodoulou, D. C. *et al.* 5′RNA-Seq identifies Fhl1 as a genetic modifier in cardiomyopathy. *J Clin Invest* **124**, 1364–1370, doi:10.1172/JCI70108 (2014).

Acknowledgments

We thank Dr. Andrew R. Marks (Columbia University Medical Center) for critical reading of the manuscript and valuable suggestions. This work was supported by grants from the National Basic Research Program of China (2011CB809104 to GJ, 2013CB531103 to XH), the American Heart Association (13POST16810041 to GS) and the National Foundation of Sciences and Technology (31271228 to GJ).

Author contributions

Q.Y., Z.C. and Z.Q.Y. designed and performed experiments; Q.Y. and G.S. designed experiments, analyzed data, and wrote the manuscript; L.G. and Z.G.Y. and Y.T.Z., performed experiments; H.B.X. and K.Y.D. generated the Calstabin2 KO and TG mice; S.Q.W. and G.J. designed experiments, analyzed data and wrote the manuscript. All authors have read and approved the final manuscript.

Additional information

Supplementary information accompanies this paper at http://www.nature.com/scientificreports

Competing financial interests: The authors declare no competing financial interests.

How to cite this article: Yuan, Q. *et al.* Functional Role of Calstabin2 in Age-related Cardiac Alterations. *Sci. Rep.* **4**, 7425; DOI:10.1038/srep07425 (2014).